ISME

Iranian Journal of Mechanical Engineering
The Iranian Society of Mechanical Engineers
Research Paper

DOI: 10.30506/JMEE.2022.552079.1288
DOR: 20.1001.1.16059727.2022.23.2.6.5

Theoretical Study of Effective Parameters in the Friction Reduction by Ultrasonic Vibrations in Solid Surfaces

A. Fattahi Avati[*]
M.Sc. of Mechanical Engineering

M.R. Karafi[†]
Assistant Professor of Mechanical Engineering

Ultrasonic vibrations are used in many fields to reduce friction forces. In this paper, the reasons for reducing friction in solid surfaces are investigated using the friction model of Dahl and the elastic-plastic contact model. Based on the theoretical model, four parameters: relative velocity, contact surface, the distance between surfaces, and Young modulus, are effective in the frictional force reduction. This study is validated using experimental tests. The results showed that the effects of oscillations of the relative velocity and changes of contact surfaces on the friction reduction are 51% and 12%, respectively. The minimum effect, among the factors, was related to the Young modulus with a value of 1%. The reason for the force reduction is the nonlinear behavior of the contact surface, contact stiffness, and the friction force functions. Moreover, fluctuations in their input parameters cause an asymmetric oscillation in the value of those functions. This feature changes these functions' average value and reduces the friction forces.

Keywords: Ultrasonic, Friction, Dahl Model, Elastic-plastic Contact.

1 Introduction

Today, the use of ultrasonic waves in different industries has progressed extensively. The applications of the ultrasonic waves include medicine, cleaning, welding of metals and plastics, wastewater purification, food industry, ultrasonic sewing, cutting process, stress-relief of industrial components, forming processes, fluid spray in the production of semiconductors, homogenizers, and so forth.
An important application of ultrasonic vibrations is friction force reduction. When two objects slip on a surface, the asperities of both surfaces are engaged, and friction is produced. The sliding friction force between two objects is reduced as the ultrasonic vibrations are applied. This property is significant in machining and forming processes. For example, ultrasonic vibrations are used to reduce the friction of chips and cutting tools, which decreases the force and temperature of cutting tools; besides, the stability of machining processes and the quality

[*] M.Sc. of Mechanical Engineering, Faculty of Mechanical Engineering, Tarbiat Modares University, Tehran, Iran
[†] Corresponding Author, Assistant Professor of Mechanical Engineering, Faculty of Mechanical Engineering, Tarbiat Modares University, Tehran, Iran, karafi@modares.ac.ir

Receive: 2022/04/17 Accepted: 2022/11/06

of machining surface are increased [1]. Zhu et al. [2] investigated the effect of ultrasonic vibrations on the plasticity of metals during the compression test. The titanium and aluminum metals are used for the tests. They observed that the amplitude and frequency of vibrations affect the plasticity of the metals; however, the lower frequency has a higher effect of "acoustic softening." If contacting surfaces are placed under a microscope, it can be seen that the surfaces have some asperities, and friction is created as these asperities are engaged. When the asperities are engaged, they undergo a deformation that can be elastic, elastic-plastic, or fully plastic. The first attempt in the field of roughness deformation was made by Greenwood et al. [3]. They modeled the contact between a rough surface and a solid surface without asperities, and an elastic model was presented for defining the deformation of asperities. Chang et al. [4] developed the Greenwood model and presented an elastic-plastic model for the deformation of asperities. Polycarpou et al. [5] presented an elastic-plastic model for the deformation of asperities which was more accurate than other models. A theoretical and experimental study was performed by Littmann et al. to investigate the effect of longitudinal and transverse ultrasonic vibrations of the frictional force [6]. They obtained a relation between the relative velocity of two objects and the friction coefficient. Leus and Gutowski [7] examined the Coulomb and the Dahl models for Littmann tests. They observed that the results of the Dahl model have a better agreement than the Coulomb model. Adachi et al. [8] investigated the friction micro-mechanism in the presence of ultrasonic waves. In their tests, oscillation motions, both circular and linear concerning a rotating disc, were considered, and they concluded that with increasing the rotational speed of the disc, the friction between surfaces would increase. Besides, by increasing the oscillation amplitude, the friction force is decreased. They reported that in oscillations with low amplitude, the disc's rotational speed has no significant effect on the friction force. In 2014, Dang and Dapino [9] experimentally and theoretically studied the effect of double-way ultrasonic vibrations (longitudinal and transverse directions) on the friction force between two objects. They obtained the friction force between aluminum and steel objects under a determined vibration amplitude and normal force. The results showed that the friction force in the presence of two-way ultrasonic vibrations has reduced up to 60%.
In this paper, Dahl's friction model, and the cubic elastic-plastic contact model, were used to estimate the friction force in the presence of ultrasonic vibrations. The effects of oscillation terms on the friction force, contact stiffness, and contact surface functions have been examined. Then the reasons for friction force reduction were studied mathematically. Besides, the effect of reduction of Young modulus has been included in the friction model. Finally, the effect of each of these parameters on the friction force reduction is investigated.

2 Theoretical Model

When two objects are in contact and slip/roll on each other, a resistant force in the opposite direction, called friction, is created. Different phenomena are observed in friction between two surfaces, each affecting the complexity of frictional models that can take them into account. Dahl model is one of these frictional models. Dahl described the behavior of the friction phenomenon by using the strain-stress diagram. For two bodies slip on each other with small displacement, he observed that the body returns to its initial position. Dahl compares this behavior with the material property in the elastic region. With further displacements of two surfaces, plastic deformation occurs. The maximum force obtained in the force-displacement diagram is called adhesion force. For soft materials, the pre-rupture force decreases as the displacement increases [10]. The friction force using the Dahl model is defined as follows:

$$F_t = \sigma\delta \tag{1}$$

Where δ is displacement, it is obtained from the following differential equation:

$$\dot{\delta} = V - \frac{\sigma\delta}{F_C}|V| \tag{2}$$

Where V denotes the relative velocity between two objects and σ is the tangential contact stiffness obtained from contact models. The tangential contact stiffness can be calculated by the cubic model as follows [9]:

$$\sigma = \frac{E\,A_r^2}{d^3} \tag{3}$$

Where A_r, and d represent the contact surface of all asperities, and surfaces distance, respectively. Besides, E is Young modulus calculated by Eq. (4):

$$\frac{1}{E} = \frac{1-\upsilon_1^2}{E_1} + \frac{1-\upsilon_2^2}{E_2} \tag{4}$$

Where E_1 and E_2 are the Young modulus of two surfaces and υ_1 and υ_2 are their corresponded Poisson's ratio, respectively.

When two surfaces are in contact, two main planes can be defined. One is the average height of asperities, and the other one is the average height of the plane on which asperities exist. Fig. (1) shows the specifications of these two planes. The upper plane (base plane) is considered solid without any asperities in this figure.

According to Fig. (1), z is the asperities height, and d is the distance of surfaces (which measures from the base plane to the average height of asperities). Besides, R denotes the radius of asperities, and h is the distance of surfaces defined from the base plane to the average height of the plane. The total number of asperities is equal to:

$$N = \eta A_n \tag{5}$$

Where A_n is the nominal contact surface and η is the density of asperities, measured experimentally. The total number of asperities on the contact surface is defined as follows:

$$N_c = N\int_d^{\infty}\phi(z)dz \tag{6}$$

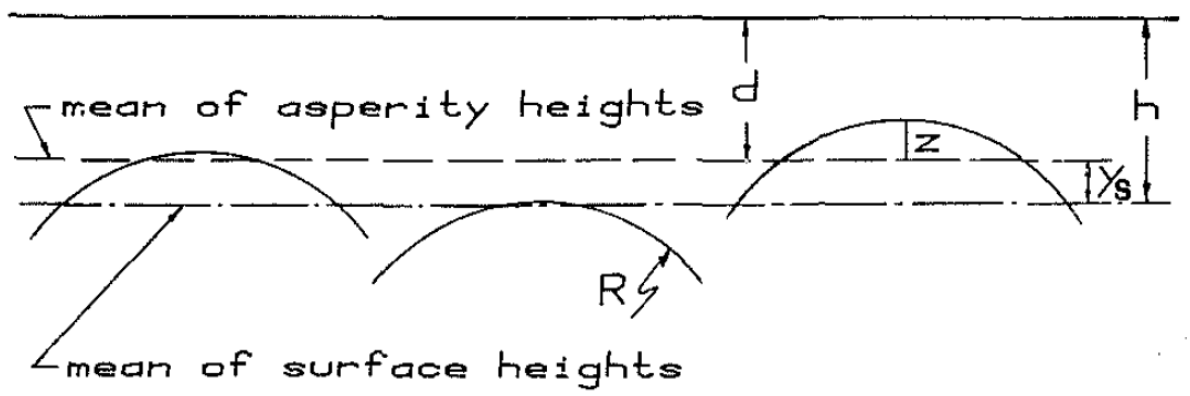

Figure 1 Asperities planes [4]

Where $\phi(z)$ is the distribution function of asperities height and is considered a Gaussian distribution. The limits of integral, (d, ∞) are considered from the positive interference of asperities on the surface of the base plane. The interference is expressed by:

$$\omega = z - d \tag{7}$$

According to Hertz's theory of contact, the area between two asperities is calculated by Eq. (8) [3]:

$$A(\omega) = \pi R \omega \tag{8}$$

The vertical force between two asperities is:

$$P(\omega) = \frac{4}{3} E^{\frac{1}{2}} R^{\frac{1}{2}} \omega^{\frac{3}{2}} \tag{9}$$

The maximum contact pressure between two asperities is defined by Eq. (10).

$$p_m = \frac{3}{2} \frac{\bar{P}}{\bar{A}} = \left(2E/\pi\right)\left(\omega/R\right)^{1/2} \tag{10}$$

From equation 10, ω can be expressed as follows:

$$\omega = \left(\frac{\pi p_m}{2E}\right)^2 R \tag{11}$$

Kohn et al. [11] defined the maximum contact pressure, p_m at the beginning of plastic deformation as follows:

$$p_m = C_\upsilon (1 - \upsilon^2) Y \tag{12}$$

By substituting Eq. (12) in Eq. (11), the critical interference is obtained from Eq. (13).

$$\omega_c = \left(\frac{\pi C_\upsilon (1 - \upsilon^2) Y}{2E}\right)^2 R \tag{13}$$

Where υ, R, Y, and E are the Poisson's ratio of softer material, the radius of the asperity, yield strength of softer material, and combined Young modulus of two objects, respectively. It should be noted that C_υ is a function of υ which is obtained using the following equation:

$$C_\upsilon = 1.234 + 1.256\upsilon \tag{14}$$

Chang et al. [4] have developed the Greenwood relation and obtained some relations for calculating plastic area and the force between two asperities. The area affected by plastic deformation between two asperities is defined as follows:

$$\bar{A} = \pi R\omega \left(2 - \frac{\omega_c}{\omega}\right) \tag{15}$$

The contact load of asperities is equal to:

$$\bar{P} = \pi R\omega \left(2 - \frac{\omega_c}{\omega}\right) p_m \tag{16}$$

Polycarpou et al. [5] presented a model for the elastic-plastic deformation of asperities, which was more accurate than the previous models. They used a modified exponential function for asperities height distributions, shown in Eq. (17).

$$\phi^*(z) = ce^{-\lambda z} \tag{17}$$

Where c and λ are constants with values of 3 and 17, respectively. The exponential distribution function is very similar to the Gaussian distribution function. Polycarpou et al. [5] stated that if the asperity deformations are elastic, the contact surface area can be obtained using Eq. (18):

$$A_e = \eta A_n \pi R R_q \int_d^{d+\omega_c} (z-d)\phi^*(z)dz \tag{18}$$

For elastic-plastic conditions, using Eqs. (15) and (16), the contact surface area is calculated as follows:

$$A_p = \eta A_n \pi R R_q \int_{d+\omega_c}^{\infty} [2(z-d) - \omega_c]\, \phi^*(z)dz \tag{19}$$

Where R_q is the standard deviation of height of asperities. By solving Eq. (18), the real contact area is obtained from the elastic deformation of asperities.

$$A_e = \frac{c\pi\beta A_n}{\lambda^2}\left[1 - (1 + \frac{\lambda\omega_c}{R_q})e^{\frac{\lambda\omega_c}{R_q}}\right] e^{-\lambda\frac{d}{R_q}} \tag{20}$$

Where $\beta = \eta R R_q$ and A_n is the nominal contact area. By solving Eq. (19), the real contact area is obtained from the plastic deformation of asperities using the following equation:

$$A_p = \frac{c\pi\beta A_n}{\lambda^2}\left(2 + \frac{\lambda\omega_c}{R_q}\right) e^{-\lambda\frac{(d+\omega_c)}{R_q}} \tag{21}$$

The real contact area, (A_r), is calculated using Eq. (22).

$$A_r = A_e + A_p \tag{22}$$

Finally, the friction force is obtained as follows:

$$F_t = \sigma\delta = \frac{\sigma V F_c}{\sigma|V|}\left(1 - e^{-\frac{\sigma|V|t}{F_c}}\right) = \frac{F_c - F_c e^{-\frac{EA_r^2 Vt\, sgn(V)}{F_c\, d^3}}}{sgn(V)} \quad (23)$$

Where, F_c is the Coulomb friction force obtained from experiments.

3 Examining Parameters

Considering that many researchers have experimentally studied the friction reduction phenomenon in the presence of ultrasonic vibrations, in the present research, the experimental results of the previous research are used to validate the theoretical model. The reference experimental results [9] validate the Dahl model. The parameters used in the experimental test of reference [9] are listed in Table (1).
As it is evident in Eq. (23), by assuming a constant value for the Coulomb friction force, F_c (according to the Dahl model), four parameters, including velocity (V), contact area (A_r), Young modulus (E), and surfaces distance (d) affecting the friction force.
The oscillation frequency of 20 kHz is used to compare the results of the present study with those of reference [9]. According to the literature survey, the maximum reduction in Young modulus by applying ultrasonic oscillations is 30%. This reduction is considered for the part connected to the transducer (first body). The normal oscillation amplitude value (d) was reported to be 1.1μm.

3.1 Velocity

If the velocity between two bodies increases, the relative displacement of two bodies increases. Increased displacement in the Dahl model means the increase of strain; besides, in the force-displacement diagram, this means an increase of force between two bodies. However, based on the Dahl model, the increase in force cannot exceed the Coulomb force due to separations of asperities. The relative velocity between two bodies is defined as follows:

$$V = V_2 + V_1 cos(2\pi f t) \quad (24)$$

Table 1 Specifications and performance conditions in reference [9]

symbol	Parameter	Value	Unit
R_q	The standard deviation of asperities height	6	μm
R	The average radius of asperities	1.7	μm
η	Density of asperities	$47*10^9$	$1/m^2$
A_n	Nominal contact surface	$1*10^{-4}$	m^2
E_1	modulus of the first object	71.3	GPa
E_2	Young modulus of the second object	200	GPa
υ_1	Poisson's ratio of the first object	0.33	-
υ_2	Poisson's ratio of the second object	0.29	-
Y	Yield strength	410	MPa
V_2	Constant relative velocity	0.005	m/s
V_1	Longitudinal vibration amplitude	1.4	m/s

Where V_1 is the velocity amplitude of the first body, V_2 is the constant velocity of the second body, and f is the vibration frequency. By substituting Eq. (24) in Eq. (23), the following equation is derived for friction force.

$$F_t = \frac{F_c - F_c e^{-\frac{EA_r^2(V_2+V_1 cos(2\pi ft))t\ sgn(V_2+V_1 cos(2\pi ft))}{F_c\ d^3}}}{sgn(V_2 + V_1 cos(2\pi ft))} \quad (25)$$

Where the value of Coulomb force is 55N and the initial value for d is $14\mu m$. Figs. (2) and (3) show the friction force in terms of the velocity (V_2) for 0.005m/s and 0.5m/s based on the Dahl model, respectively. The figures reveal that increasing the relative velocity makes the friction force reaches its maximum value faster.

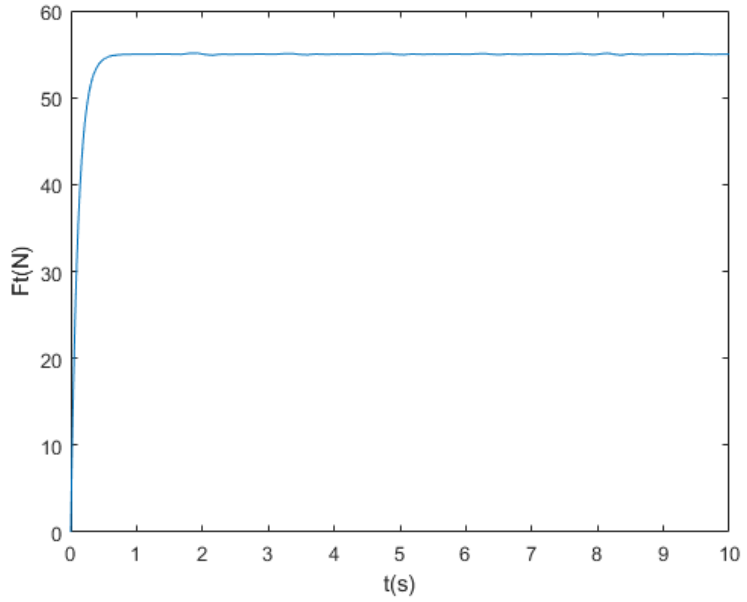

Figure 2 Friction force in terms of time for the constant velocity of 0.005m/s

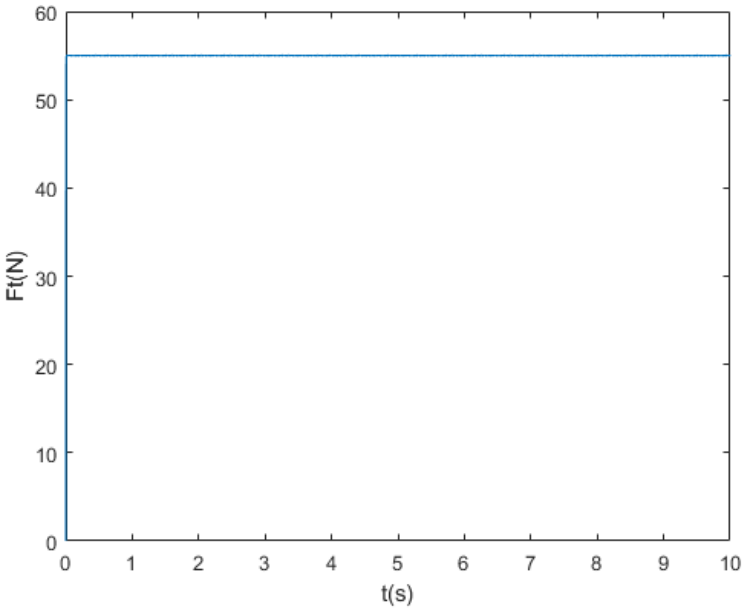

Figure 3 Friction force in terms of time for the constant velocity of 0.5m/s.

By applying ultrasonic vibrations, the relative velocity between two surfaces (V) varies in an oscillation form. The effect of velocity changes on the friction force is depicted in Figs. (4)-(6). The values of parameters d, A_r, and E are considered constant in these figures.
It can be seen from Fig. (5) that by decreasing the constant velocity component, the effect of oscillations is increased. In this case, the average friction force is decreased.
This figure shows that with increasing the vibration amplitude, concerning the constant velocity of two bodies, the effect of oscillation is increased.

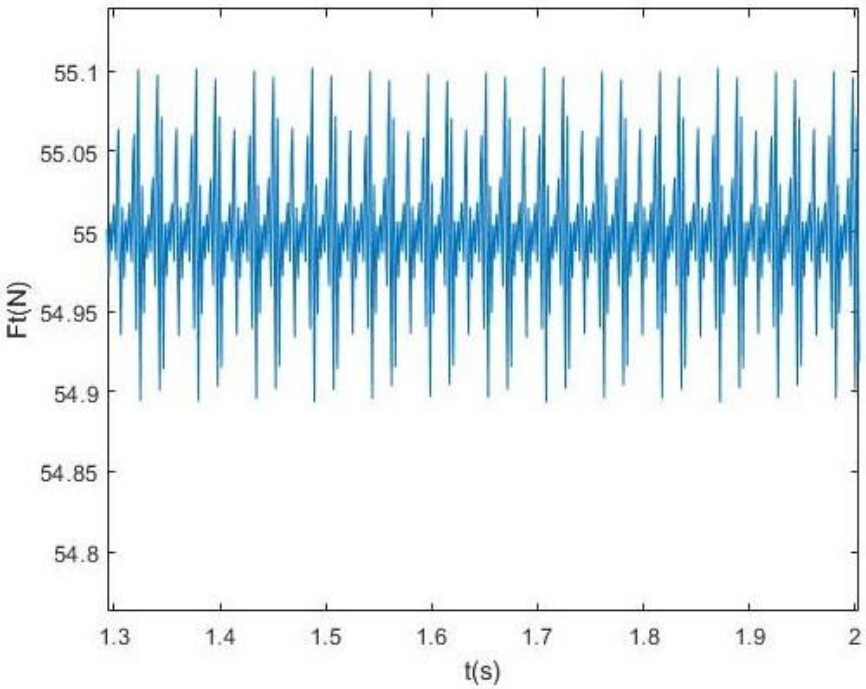

Figure 4 Friction force in terms of time for the constant velocity of 0.5m/s, amplitude of vibration velocity of 1.4m/s, and frequency of 20 kHz.

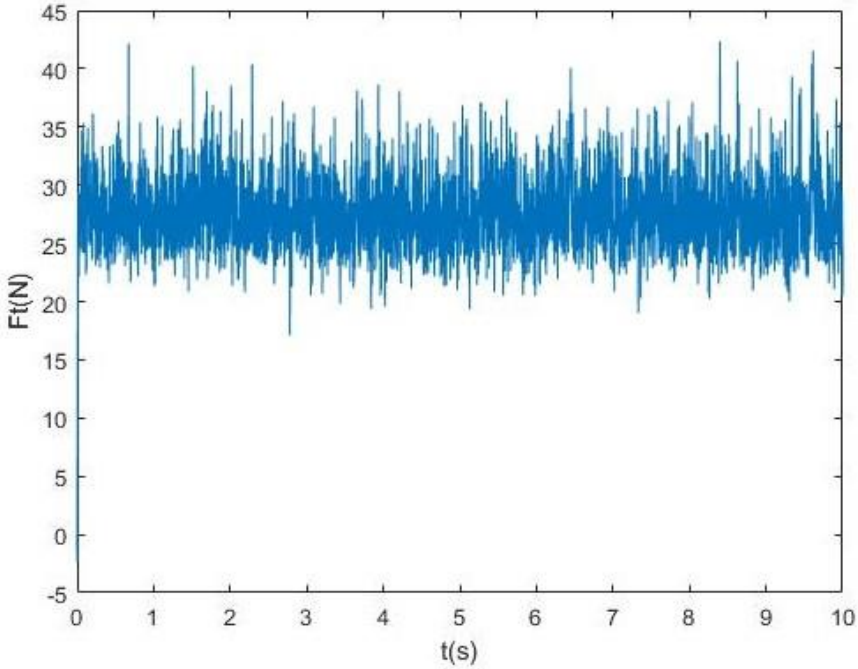

Figure 5 Friction force in terms of time for the constant velocity of 0.005m/s, amplitude of vibration velocity of 1.4m/s, and frequency of 20 kHz

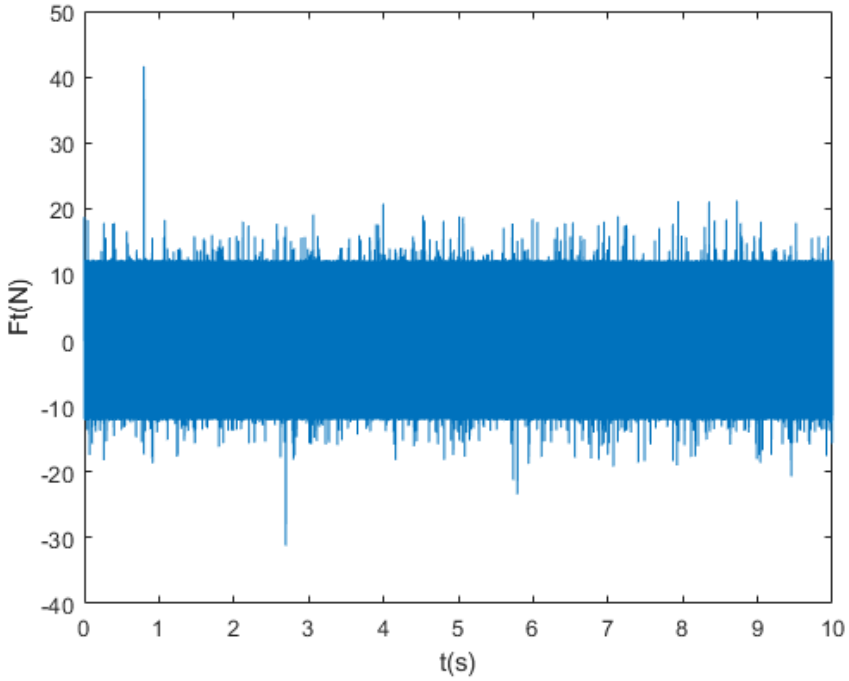

Figure 6 Friction force in terms of time for the constant velocity of 0.005m/s, amplitude of vibration velocity of 14.5m/s, and frequency of 20 kHz

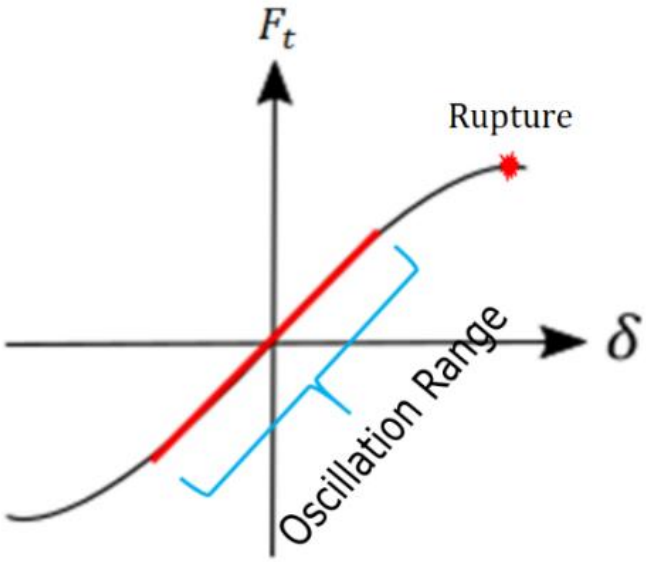

Figure 7 Velocity oscillations and their effect on the friction force reduction

According to the modeling results, applying oscillation velocity and back and forth motion on the force-displacement diagram is one reason for reducing the friction force by ultrasonic vibrations. Such motion leads to a reduction in the average friction force. Fig. (7) shows the effect of displacement (velocity) oscillations on the friction force.

3.2 Contact surface

The transverse vibrations are applied to the surface due to the Poison effect by applying the longitudinal ultrasonic vibrations. Therefore, the height of asperities will increase/decrease; as a result, the contact surface increases/decreases. This section investigates the effect of friction

force reduction by applying the transverse vibrations of $1.1\mu m$, assuming constant Young modulus and velocity. Firstly, the effect of parameter d on the effective contact surface of two bodies is studied. Fig. (8) shows that the contact surface decreases exponentially with increasing the parameter d. Eq. (22) has been used to plot this curve.

According to the fig. (8), for $d_0 = 14\ \mu m$, the value of the contact surface is $1.397 \times 10^{-7} m^2$. The average value of the contact surface after applying the oscillations with an amplitude of 1.1 μm is reduced by 4% and reaches $1.341 \times 10^{-7} m^2$.

Then, the effect of d on the contact stiffness is investigated. As shown in Fig. (10), this parameter significantly affects the contact stiffness, a part of which is due to the reduction in the contact area.

The function A_r in terms of d exhibit nonlinear behavior. Thus, the variations of parameter d lead to an asymmetrical oscillation around the equilibrium point, which reduces its average value. This reduction trend is depicted in Fig. (9).

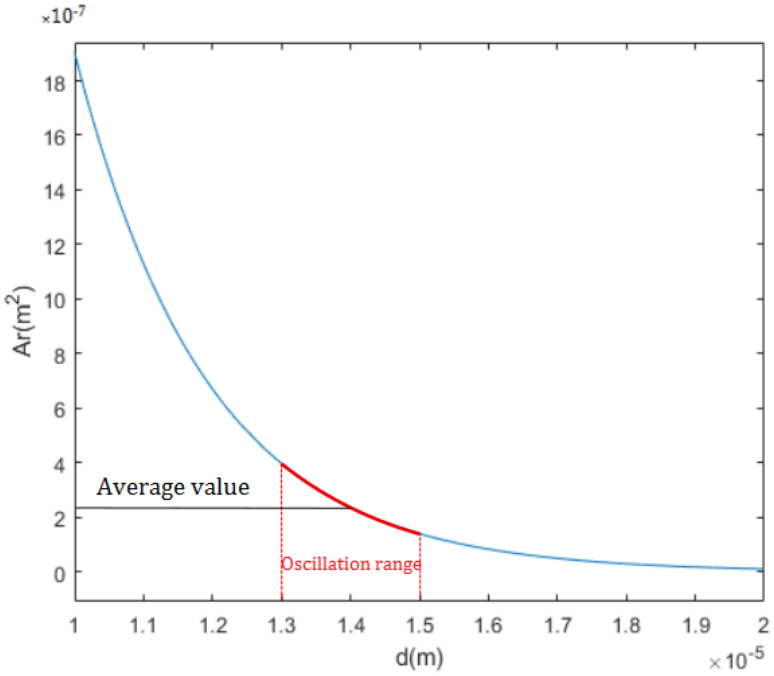

Figure 8 Variation of the effective contact surface in terms of parameter d

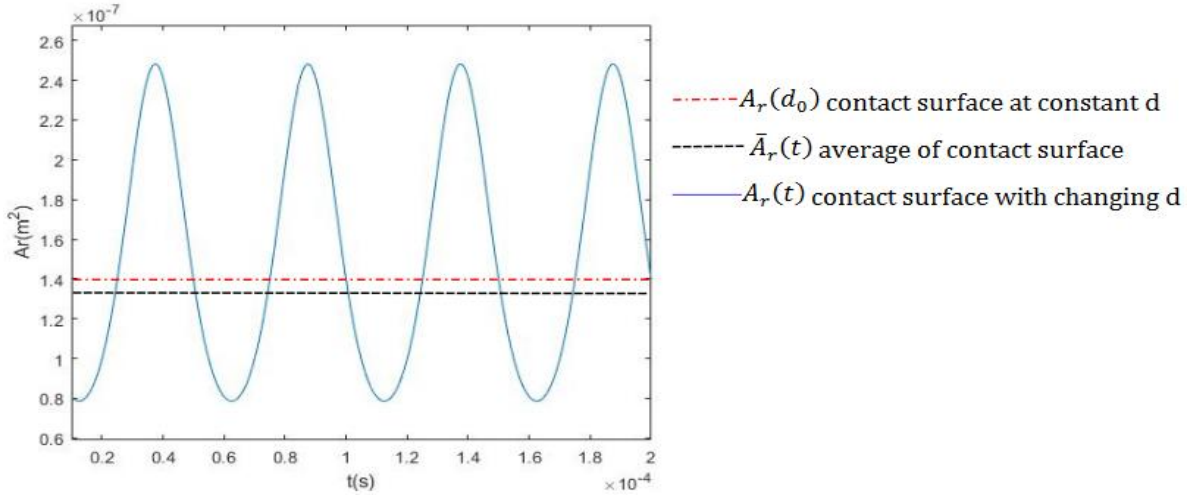

Figure 9 Contact area function in terms of changing the parameter d

The function has a nonlinear behavior in terms of d parameter. Thus, the variations of this parameter lead to an asymmetric oscillation around the equilibrium point; as a result, its mean value is reduced. This reduction is represented in Fig. (11).
According to Fig. (10), for $d_0 = 14\ \mu m$, the value of tangential contact stiffness is $2.326 \times 10^{11} N.m^{-1}$. By applying the oscillations with an amplitude of 1.1 μm, the average value of tangential contact stiffness is reduced by 11% and reaches $2.07 \times 10^{-7} N.m^{-1}$. The nonlinear behavior of friction force in terms of d parameter is depicted in Fig. (12).
Fig. (13) shows how the average friction force decreases as the oscillations are applied.

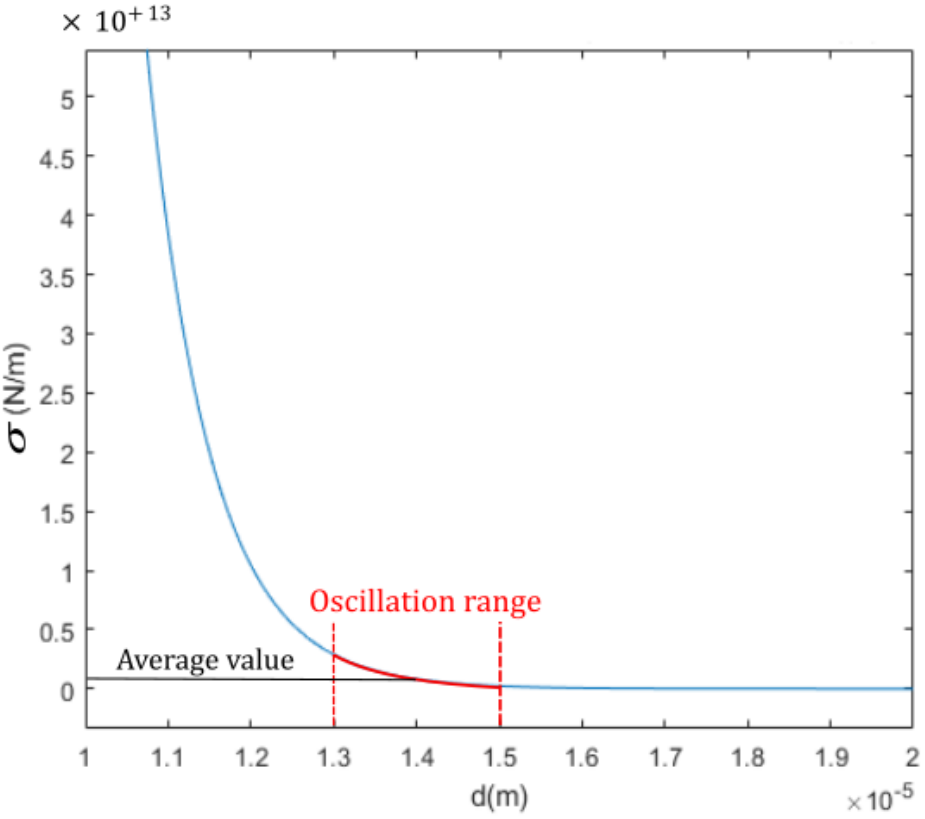

Figure 10 Tangential contact stiffness in terms of d parameter

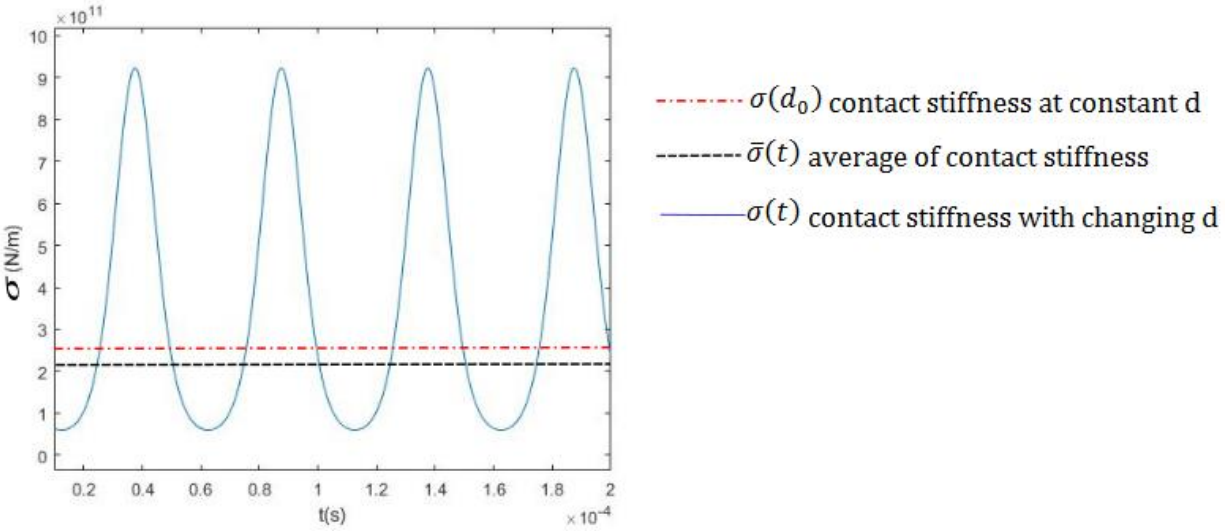

Figure 11 Tangential contact stiffness curve in terms of time

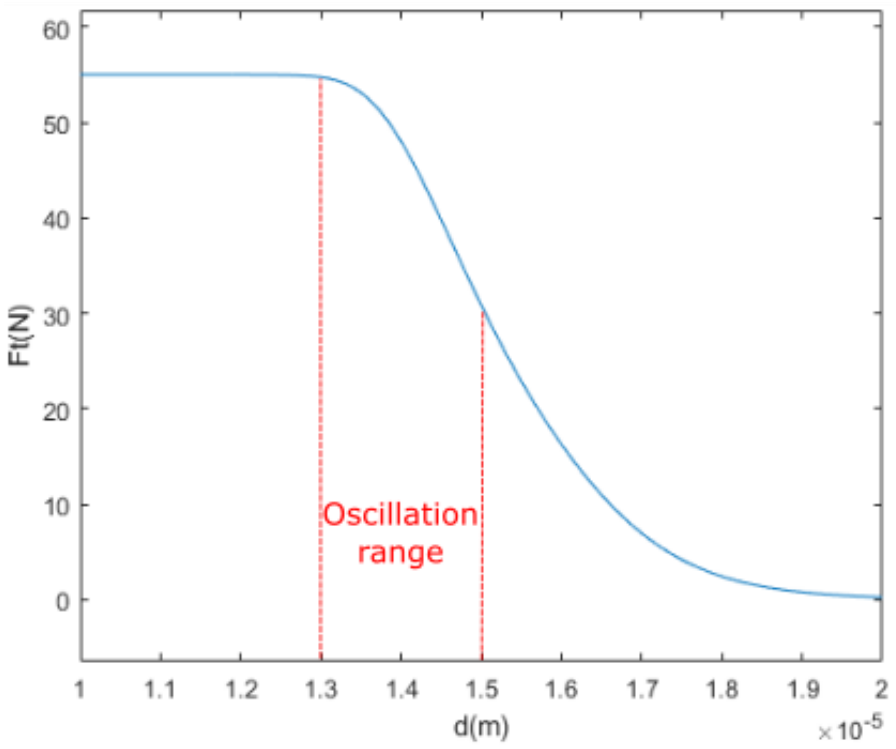

Figure 12 Friction force curve in terms of d parameter.

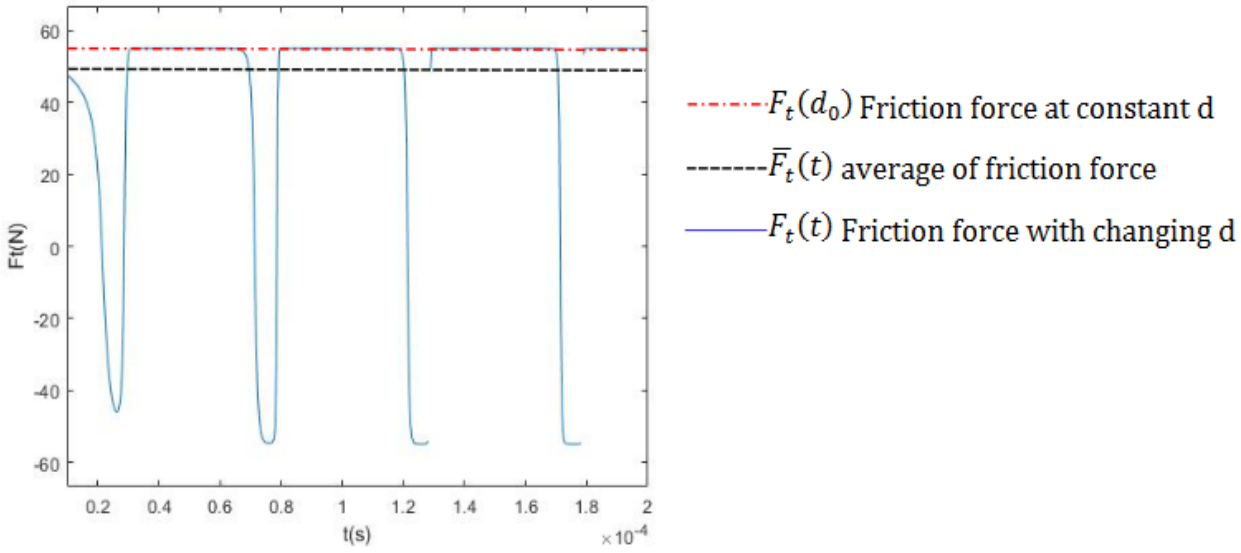

Figure 13 Friction force curve in terms of time

According to Fig. (13), for $d_0 = 14\ \mu m$, the value of friction force is $55N$. By applying the oscillations with an amplitude of 1.1 μm, the average value of friction force is reduced by 12% and reached $48N$. Based on the Figs. (8) through (13), it can be concluded that one reason for the friction force reduction is the nonlinear behavior of contact stiffness, and the contact surface.

3.3 Young Modulus

The acoustic softening is occurred in metals, such as steel and aluminum, by applying ultrasonic vibrations. This phenomenon leads to a reduction of the Young modulus [4, 13, and 14]. Fig. (14) shows the experimental results of ultrasonic vibrations on the aluminum.

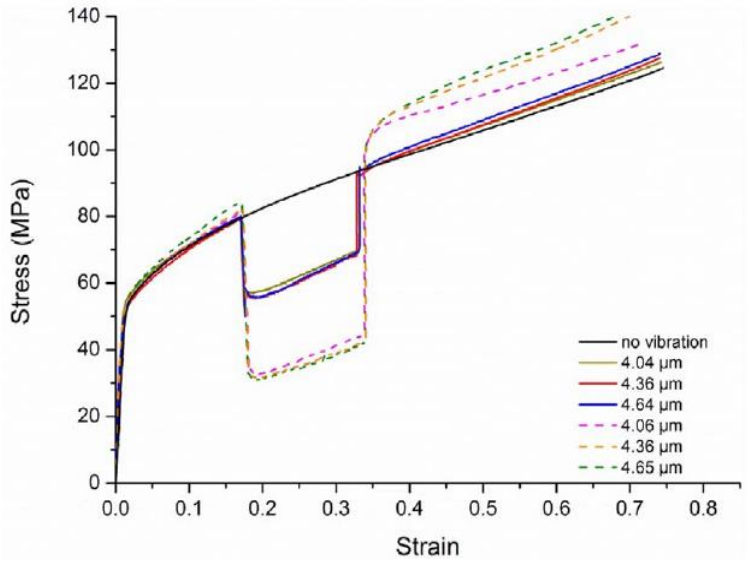

Figure 14 Effects of ultrasonic vibrations on the plasticity of aluminum [2], Dash line: frequency of 30 kHz; solid line: frequency of 40 kHz.

According to Eq. (3), the contact stiffness is reduced with decreasing Young modulus. The reduction of Young modulus may be due to temperature rise and/or the increase in intermolecular distances due to the ultrasonic vibrations. In the friction model, the temperature effect is not considered; however, the reduction of the Young modulus affects the friction force. Based on the calculations, the maximum effect of the Young modulus on the friction force reduction is 1%.

3.4 Results and Discussion

Table (2) lists the contribution of each parameter to the friction force reduction. In tests, No. 1 through 5, the transverse vibrations amplitude and the oscillation velocity amplitude of reference [9] are used. It should be noted that test, No. 6, is the hypothetical test conducted in the present research.

The value of the friction force before applying the ultrasonic vibrations was the same, 55N, both in the experimental test and the theoretical analysis. Regarding all parameters, a 62% reduction was observed in the friction force (reaching 21N). By reducing the transverse vibrations to $0.9\mu m$, and the velocity oscillations amplitude to$115 \times 10^4 \mu m$, the value of friction force was 28N, representing great agreement with the experimental value. The difference in the vibrations' amplitude may be due to the measurement error reported in reference [9].

Table 2 Effect of each parameter on the friction force reduction

Test No.	Young modulus reduction, %	Transverse oscillation amplitude, μm	Oscillation velocity amplitude, μm/s	The calculated friction force, N	Friction force reduction, %
1	-	-	-	55	0
2	30	1.1	$144*10^4$	21	62
3	-	-	$144*10^4$	27	51
4	-	1.1	-	48	12
5	30	-	-	54	1
6	30	0.9	$115*10^4$	28	49

4 Conclusion

The elastic-plastic contact and Dahl friction models have been used, and it was concluded that relative velocity, contact surface, the distance of surfaces, and Young's modulus affect the friction force reduction under ultrasonic vibrations. The velocity oscillations have the maximum effect. Besides, the contact surface and reduction of Young modulus are, respectively, the second and third parameters with maximum effect. The experimental tests were used to validate the analytical model. In this research, ultrasonic vibrations caused a 62% reduction in friction force. Based on the modeling results, the oscillation velocity and back-and-forth motion on the force-displacement curve are the most influential parameters in friction reduction. The effect of velocity oscillations is approximately 51%. The results revealed that the transverse vibrations with an amplitude of $1.1\mu m$ caused a reduction of 4% in the contact surface. In addition, variations of the contact surface and surface distance caused a 12% reduction in friction force. Also, the contribution of the contact stiffness and young modulus were 11% and 1%, respectively.
Mathematically, the nonlinear behaviors of friction force, the contact surface, and contact stiffness functions lead to an asymmetric oscillation in the value of those functions. This property leads to a reduction in the average value of this function when the oscillations are applied.

5 Ethical Approval

Not applicable.

6 Consent to Participate

Not applicable.

7 Consent to Publish

Not applicable.

8 Authors' Contributions

Mohammad Reza Karafi is a supervisor of the research. He interprets the models and revises the manuscript. Ali Fattahi conducted experiments and performed calculations, and prepared the manuscript.

9 Funding

The authors received no financial support for the research.

10 Competing Interests

We declare that we have no significant competing financial, professional, or personal interests that might have influenced the performance or presentation of the work described in this manuscript.

11 Availability of Data and Materials

Raw data were generated at Metrology and Advanced Mechatronics Laboratory, faculty of mechanical engineering, Tarbiat Modares University, Tehran, IRAN. Derived data supporting the findings of this study are available from the corresponding author on request.

12 Code availability

Matlab codes used in this research are available from the corresponding author on request.

References

[1] Voronina, S., and Babitsky, V., "Autoresonant, Control Strategies of Loaded Ultrasonic Transducer for Machining Applications", Journal of Sound and Vibration, Vol. 313(3-5), pp. 395-417, (2008).

[2] Zhou, H., Cui, H., and Qin, Q.H., "Influence of Ultrasonic Vibration on the Plasticity of Metals During Compression Process", Journal of Materials Processing Technology, Vol. 251, pp. 146-159, (2018).

[3] Greenwood, J.A., and Tripp, J.H., "The Elastic Contact of Rough Spheres", Journal of Applied Mechanics, Vol. 34(1), pp.153-159, (1967).

[4] Chang, W.R., Etsion, I., and Bogy, D.B., "An Elastic-plastic Model for the Contact of Rough Surfaces, Journal of Tribology, Vol. 109(2), pp. 257-263, (1987).

[5] Polycarpou, A.A., and Etsion, I., "Analytical Approximations in Modeling Contacting Rough Surfaces, Journal of Tribology, Vol. 121(2), pp. 234-239, (1999).

[6] Littmann, W., Storck, H., and Wallaschek, J., "Reduction of Friction using Piezoelectrically Excited Ultrasonic Vibrations", In Smart Structures and Materials 2001: Damping and Isolation, International Society for Optics and Photonics, Vol. 4331, pp. 302-311, (2001).

[7] Leus, M., and Gutowski, P., "Analysis of Longitudinal Tangential Contact Vibration Effect on Friction Force using Coulomb and Dahl Models, Journal of Theoretical and Applied Mechanics, Vol. 46(1), pp. 171-184. (2008).

[8] Adachi, K., Kato, K., and Sasatani, Y., "The Micro-mechanism of Friction Drive with Ultrasonic Wave", Wear, Vol. 194(1-2), pp. 137-142, (1996).

[9] Dong, S., and Dapino, M.J., "Elastic–plastic Cube Model for Ultrasonic Friction Reduction via Poisson's Effect, Ultrasonics, Vol. 54(1), pp. 343-350, (2014).

[10] Dahl, P.R., "A Solid Friction Model", Technical Report, Accession No. ADA041920, Aerospace Corp el Segundo CA, Defence Technical Information Center, (1968).

[11] Cohen, D., Kligerman, Y., and Etsion, I., "A Model for Contact and Static Friction of Nominally Flat Rough Surfaces under Full Stick Contact Condition", Journal of Tribology, Vol. 130(3), 031401 (9 pages), https://doi.org/10.1115/1.2908925, (2008).

Nomenclature

V_2	The constant velocity of the second body	$\mathrm{m/s}$
Y	Failure strength	MPa
d	Separation distance	μm
f	Frequency	Hz
p_m	Maximum contact pressure	$\mathrm{N/m^2}$
t	time	s
z	Height of asperity measured from the mean of asperity heights	μm
σ	Tangential contact stiffness	$\mathrm{N/m}$
δ	displacement	μm
η	asperity density	$\mathrm{1/m^2}$
λ	Constant coefficient	-
υ	Poisson's ratio	-
υ_1	Poisson's ratio of the first part	-
υ_2	Poisson's ratio of the second part	-
β	Roughness parameter	-
ω	Local interference	μm
ω_c	Critical interference	μm
$\phi(z)$	The distribution function of asperity heights	-
A_r	Real contact area	m^2
A_e	Elastic contact area	m^2
A_p	Plastic contact area	m^2
A_n	Nominal contact area	m^2
$\bar{A}$	The contact area of an individual asperity	m^2
C_v	Hardness coefficient	-
E	Young modulus	GPa
E_1	Young modulus of the first part	GPa
E_2	Young modulus of the second part	GPa
F_c	Coulomb friction	N
F_t	Friction force	N
N	Total number of asperities	-
N_c	Number of contacting asperity	-
$\bar{P}$	Contact load of an individual asperity	N
R	Asperity summits radius	μm
R_q	Asperity heights deviation	μm
V	Relative velocity	$\mathrm{m/s}$
V_1	Velocity amplitude of the first body	$\mathrm{m/s}$